TECHNICAL TRANSACTIONS | CZASOPISMO TECHNICZNE
MECHANICS | MECHANIKA
1-M/2016

JERZY BAŁDYGA, MAGDALENA JASIŃSKA*

FLOW STRUCTURE, DROP DEFORMATION AND MASS TRANSFER IN DENSE EMULSIONS

STRUKTURA PRZEPŁYWU, DEFORMACJA KROPEL I TRANSPORT MASY W GĘSTYCH EMULSJACH

Abstract

This paper presents applications of a new model of the rheological behaviour of dense oil-in-water emulsions of non-colloidal droplets to describe the flow structure, the effects of the flow of dense emulsion on drop deformation and the related increase of the interfacial area and the mass transfer rate.

Keywords: dense emulsions, rheology, mass transfer

Streszczenie

W artykule przedstawiono metodę wykorzystania modelu reologii gęstych emulsji olej/woda do opisu struktury przepływu, deformacji kropel, rozwinięcia powierzchni międzyfazowej oraz współczynników wymiany masy. Przedyskutowano możliwość wykorzystania podobnych metod do opisu układów micelarnych.

Słowa kluczowe: gęste emulsje, reologia, wymiana masy

DOI:

* Prof. PhD. DSc. Eng. Jerzy Bałdyga, PhD. DSc. Eng. Magdalena Jasińska, Department of Engineering and Chemical Reactors Dynamic, Faculty of Chemical and Process Engineering, Warsaw University of Technology.

1. Introduction

Dense emulsions form many useful products including food products (homogenised milk, sauces, dressings, beverages, butter), as well as pharmaceutical and cosmetic products such as creams and balms. Emulsions are used as personal hygiene products, fire-fighting agents, agricultural industry products, paints and inks. In the manufacturing and applying of emulsions, it is often necessary to predict or control the emulsion viscosity and the flow pattern. The mass transfer between the continuous and dispersed phase can also affect this process.

Emulsion viscosity η depends on the continuous phase viscosity η_c, the volume fraction of the dispersed phase ϕ and its viscosity η_d, the interfacial tension σ, the shear rate $\dot{\gamma}$, the emulsifying agent (if present) and of course, on temperatures that obviously affect the physicochemical properties. The development of strict theoretical models is possible for infinitely dilute emulsions of spherical uncharged droplets.

The equation for the relative viscosity η_r under the limiting conditions listed below, when the hydrodynamic viscous stress is negligible compared to the interfacial stress, was proposed by Taylor [1]:

$$\eta_r = \frac{\eta}{\eta_c} = 1 + \left[\frac{5 \cdot K + 2}{2 \cdot (K + 1)}\right] \cdot \phi \tag{1}$$

where $K = \eta_d/\eta_c$ is the ratio of the dispersed-phase viscosity η_d to the continuous-phase viscosity η_c and ϕ is the volume fraction of droplets. Equation (1) is valid for $\phi \to 0$, $N_{Ca} \to 0$ and $Pe \to \infty$, where N_{Ca} is the capillary number,

$$N_{Ca} = \eta_c \cdot \dot{\gamma} \cdot R / \sigma \tag{2}$$

being the ratio of the hydrodynamic stress that tends to stretch the droplet and increase its surface energy, to the interfacial tensile stress resulting from interfacial tension, σ. The tensile stress tends to decrease the surface energy by maintaining the spherical shape of the droplet. *Pe* is the Péclet number defined by

$$Pe = \frac{\dot{\gamma} \cdot R^2}{D_B^{\infty}} \tag{3}$$

where D_B^{∞} is the coefficient of Brownian diffusion for a particle separated from other particles, R is the drop radius, and $Pe >> 1$ is equivalent to the condition that the drops are much larger than the distance travelled due to Brownian motions.

Most of models on the rheology of emulsions are based on the extension of this early model proposed by Taylor. Recently, a new method was proposed for including the effect of the droplet size distribution on the rheological behaviour of dense oil-in-water emulsions of non-colloidal droplets [2]. The method is based on an extension of the advanced model [3] for the relative viscosity of the concentrated monodisperse emulsion to account for polydispersity effects.

Model [3] is constituted by Equation (4) with three parameters *M*, *N* and *P* defined by Equations (5), (6) and (7) and dependent upon the capillary number $N_{Ca} = \eta_c \cdot \dot{\gamma} \cdot R / \sigma$ and the viscosity ratio *K*.

$$\eta_r \cdot \left[\frac{M - P + 32 \cdot \eta_r}{M - P + 32} \right]^{N-1.25} \cdot \left[\frac{M + P - 32}{M + P - 32 \cdot \eta_r} \right]^{N+1.25} = \left(1 - \frac{\phi}{\phi_m} \right)^{-2.5 \cdot \phi_m} \tag{4}$$

$$M = \sqrt{\left(64 / N_{Ca}^2\right) + 1225 \cdot K^2 + 1232 \cdot \left(K / N_{Ca}\right)} \tag{5}$$

$$P = 8 / N_{Ca} - 3 \cdot K \tag{6}$$

$$N = \frac{\left(22 / N_{Ca}\right) + 43.75 \cdot K}{\sqrt{\left(64 / N_{Ca}^2\right) + 1225 \cdot K^2 + 1232 \cdot \left(K / N_{Ca}\right)}} \tag{7}$$

The model expressed by Equations (4) to (7) was validated using much experimental data starting from the paper by Pal [3]; however, effects resulting from the drop size distribution were explained in [2].

To include the polydispersity of emulsion [2] one needs to calculate the equivalent radius *R* of the polydisperse system using the drop volume distribution $f_V(R_i)$, such that $f_V(R_i)\mathrm{d}R_i$ means a volume fraction of drops from the range R_i to $R_i + \mathrm{d}R_i$.

$$I(R) = \int_0^\infty f_V(R_i) \cdot I(R_i) \mathrm{d}R_i \tag{8}$$

with $I(R_i)$ given by

$$I(R_i) = \frac{\left(4 / N_{Ca\,i}\right) \cdot \left(2 + 5 \cdot K\right) + \left(K - 1\right) \cdot \left(16 + 19 \cdot K\right)}{\left(40 / N_{Ca\,i}\right) \cdot \left(1 + K\right) + \left(2 \cdot K + 3\right) \cdot \left(16 + 19 \cdot K\right)} \tag{9}$$

where $N_{Ca\,i} = \eta_c \cdot \dot{\gamma} \cdot R_i / \sigma$.

Figure 1 shows the relative viscosity calculated using bimodal distribution; the viscosity is plotted against the capillary number based on the equivalent radius *R* that is defined by Equations (8) and (9). There are three more curves on the figure that are constructed using the capillary number based on the mean sizes R_{10}, R_{32} and R_{30} that characterise the considered population for the same relative viscosity, η_r. The difference between the curves $\eta_r = f(N_{Ca})$ is significant.

Figure 1 shows that neither of the mean sizes traditionally used to characterise population, i.e. R_{10}, R_{32} and R_{43} is able to represent the population as the characteristic size in the model for the emulsion viscosity in the case of the bimodal distribution. However, as shown in Figure 2, in the case of the bell-shaped, unimodal distribution, the curve for the capillary number defined using R_{32} represents the distribution quite well – the difference in

the predicted viscosity is less than 10% in such a case. This problem is discussed in detail in Ref. [2].

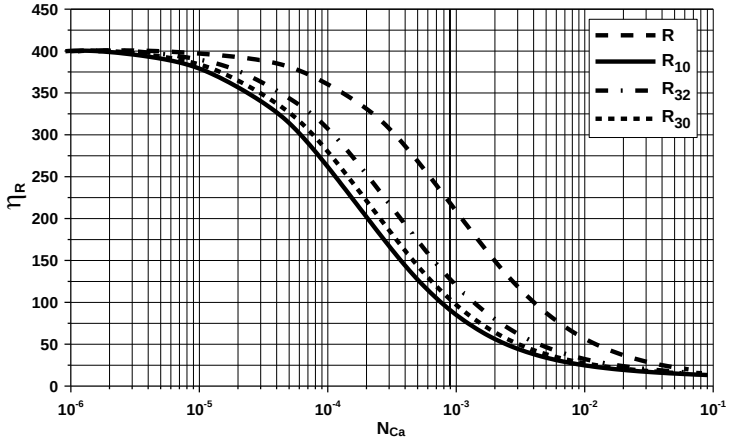

Fig. 1. Effect of the capillary number on the relative viscosity for $\phi_m = 0.8$, volume fractions of dispersed phase $\phi = 0.795$, $\eta_c = 0.91$ mPas, $\eta_d = 9.4$ mPas; bimodal distribution

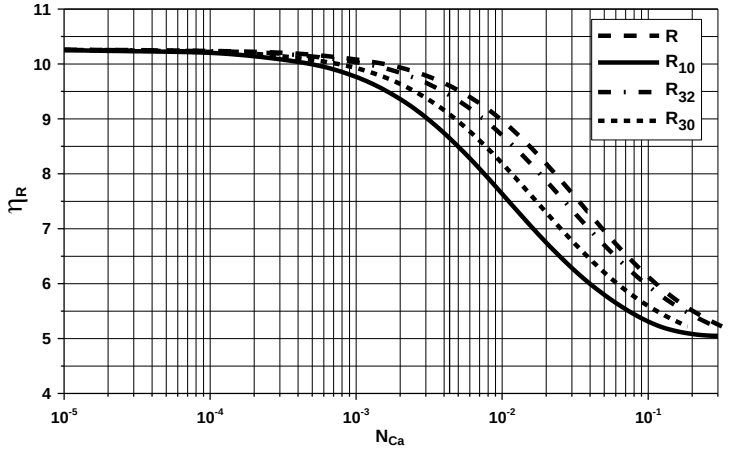

Fig. 2. Effect of the capillary number on the relative viscosity for $\phi_m = 0.8$, volume fractions of dispersed phase $\phi = 0.60$, $\eta_c = 0.91$ mPas, $\eta_d = 9.4$ mPas; unimodal distribution

As shown in Ref. [2], the model has a universal character and can be combined with the population balance equation and CFD. Examples of modelling are presented in [2] for laminar and turbulent flows of dense emulsions. In the case of laminar flow, the Couette flow and the Taylor-Couette flow were considered. In the case of turbulent flow, it has been shown how dispersion of droplets in the high-shear, rotor-stator mixer affects the flow pattern and rheology of the emulsion product.

2. Simulation of turbulent dispersion of drops in dense emulsion

To perform computations, it has been assumed that dense emulsions can be treated as the shear thinning pseudo-homogeneous fluids of the constant volume fraction of the dispersed phase of viscosity expressed by Equations (4) to (9). The local values of the drop size distribution are calculated using the moment transformation of population balance and QMOM to solve the moment balances using the breakage kernel based on the multifractal theory of turbulence as presented by Bałdyga and Podgórska [4]. The assumption of pseudo-homogeneity is supported by the observation of Ovarlez et al. [5], that no migration of droplets takes place in dense emulsions during the Couette flow. According to Ovarlez et al. [5], a reason for keeping homogeneity could be the deformability of droplets resulting from shear.

Following the results presented in [2], we consider here the dispersion of droplets present in dense emulsion in the in-line Silverson 150/250 MS high-shear, rotor-stator mixer and observe the modification of the rheological properties of the emulsion.

A performance of the Silverson double-screen mixer 150/250/MS, the same as that applied in [2] and [6], is investigated to simulate drop dispersion. The mixer is equipped with twin rotors that rotate with the same frequency within close-fitting screens. The inner rotor has an inner diameter of $2.62 \cdot 10^{-2}$ m, the outer diameter is $3.81 \cdot 10^{-2}$ m, and is equipped with four blades. The outer rotor diameters are $4.99 \cdot 10^{-2}$ m (internal) and $6.35 \cdot 10^{-2}$ m (external) and this rotor is equipped with eight blades.

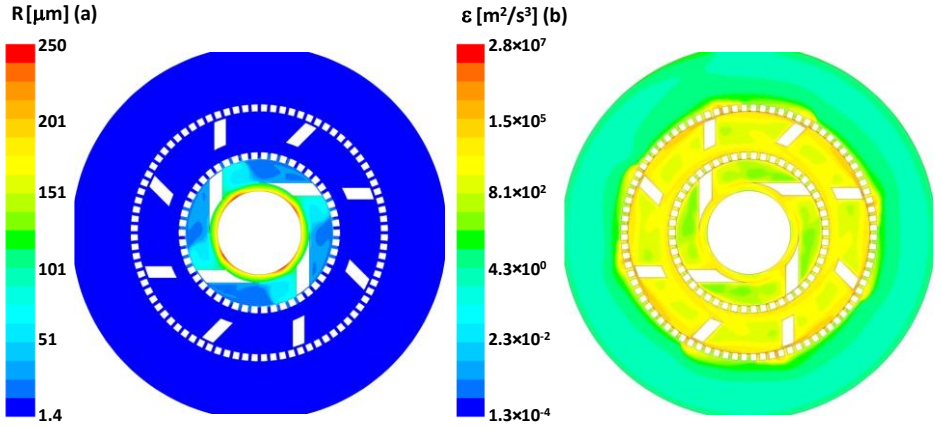

Fig. 3. Distribution of the equivalent radius (a) and the rate of energy dissipation (b) for $\phi_m = 0.8$, $\phi = 0.75$, $\eta_c = 0.91$ mPas, $\eta_d = 9.4$ mPas, Q = 600 kg/h, N = 11000 rpm

The inner stator screen has six rows of fifty circular holes each with a diameter of $1.59 \cdot 10^{-3}$ m. The inner stator screen of diameter 42.4 mm has six rows of fifty circular holes each with a diameter of $1.59 \cdot 10^{-3}$ m, (1/16 inch) on a 0.100 inch tri pitch. The outer screen, with a diameter of 67.6 mm, has seven rows of eighty circular holes each with a diameter of

$1.59 \cdot 10^{-3}$ m on a 0.100 inch tri pitch. The rotor-stator gap is 0.24 mm. In all calculations the interfacial tension was equal to 10.6 mN/m.

Figures 3 (a) and (b) show that the region of drop breakage is localised in the rotor swept region where the rate of energy dissipation is the highest. Figure 4 shows distribution of the relative viscosity in the mixer. The shear thinning properties of emulsion are very well observed. As presented in Ref. [2], the flow curves characterising the rheology of the emulsion after processing in the rotor-stator mixer under different process conditions depend on the resulting drop size distributions.

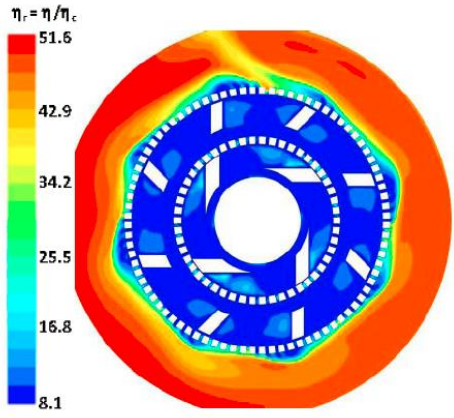

Fig. 4. Distribution of the relative, effective viscosity for ϕ_m = 0.8, ϕ = 0.75, η_c = 0.91 mPas, η_d = 9.4 mPas, Q = 600 kg/h, N = 3000 rpm

3. Drop deformation and mass transfer in dense emulsion

In the case of shear flow or extensional flow when the external viscous force is smaller than the surface tension force ($N_{Ca} < 10$), the droplets are slightly deformed. According to an analytical solution by Taylor [7], the drop is represented by an elongated sphere that can be approximated by a prolate ellipsoid, as shown schematically in Figure 5. The drop shape is then determined by Equation (10)

$$D_T = \frac{L-B}{L+B} = \frac{19+19 \cdot K}{16 \cdot (1+K)} \cdot N_{Ca} \tag{10}$$

where D_T represents the Taylor shape deformation parameter, whereas L and B are the major and minor axes of the deformed drop, respectively.

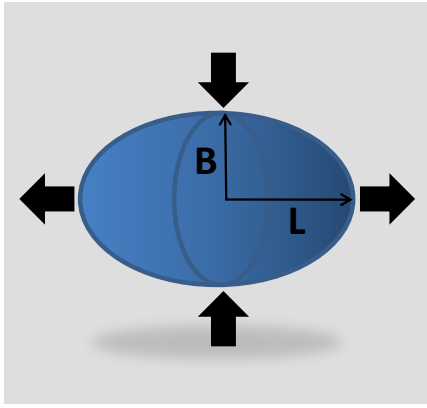

Fig. 5. Schematic of a slightly deformed drop

Combining eq. (10) with two expressions for the drop volume

$$V = \frac{4}{3} \cdot \pi \cdot B^2 \cdot L \tag{11}$$

$$V = \frac{4}{3} \cdot \pi \cdot R^3 \tag{12}$$

where R denotes the equivalent radius, one can calculate L and B, and the resulting surface area of the drop. Under the process conditions applied in this work, the drops are only slightly deformed; it can be seen in Figures 6 and 7 that increase of the specific interfacial area due to shear effect is rather small, when compared to spherical particles of the same volume.

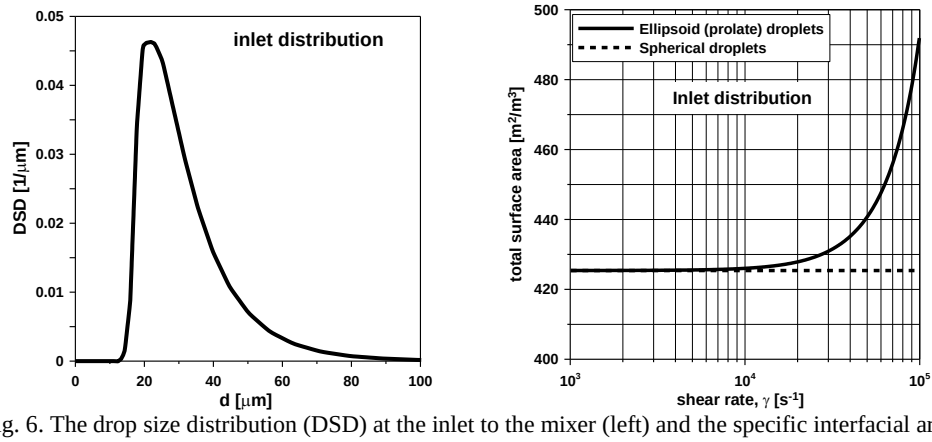

Fig. 6. The drop size distribution (DSD) at the inlet to the mixer (left) and the specific interfacial area of the feed emulsion (right)

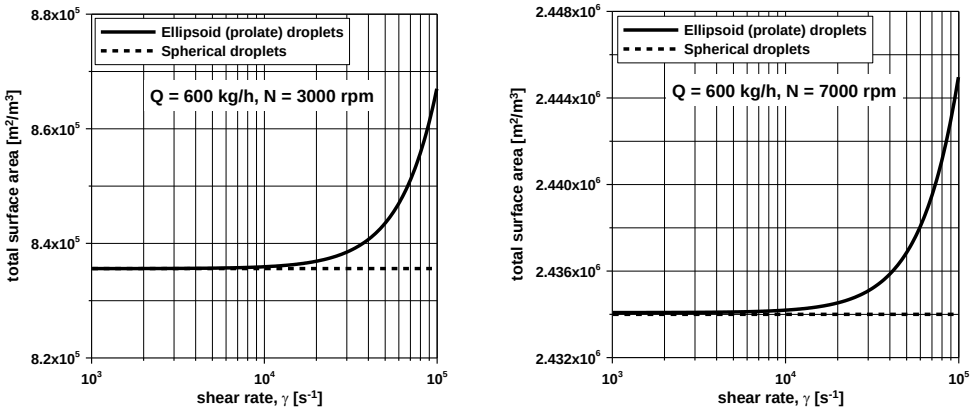

Fig. 7. The specific interfacial area after processing emulsion for ϕ_m = 0.8, ϕ = 0.75, η_c = 0.91 mPas, η_d = 9.4 mPas, Q = 600 kg/h, N = 3000 rpm and 7000 rpm, respectively

The effect of drop elongation is also observed during emulsion processing. This is presented in Figure 8.

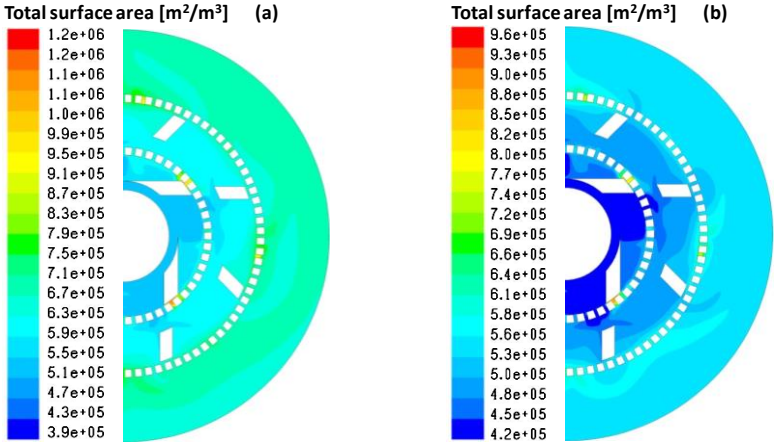

Fig. 8. The specific interfacial area during the process of creating emulsion for ϕ_m = 0.8, ϕ = 0.75, η_c = 0.91 mPas, η_d = 9.4 mPas, Q = 600 kg/h, N = 1000 rpm. (a) elongated droplets, (b) neglecting drop deformation

The model for predicting external mass transfer coefficient to or from prolate, ellipsoid drops submerged in an extensional flow was recently proposed by Favelukis and Lavrenteva [8].

$$k_L a_{drop} = 4 \cdot \pi \cdot R \cdot D_i \cdot \sqrt{\frac{3}{2 \cdot \pi \cdot (1+K)}} \cdot \left[1 - \frac{4 \cdot (4+31 \cdot K) \cdot Y}{315 \cdot (1+K)} \cdot N_{Ca} \right] \cdot Pe^{1/2} \qquad (13)$$

where $Y = (19 \cdot K + 16)/(16 \cdot K + 16)$ and in this equation, $Pe = \dot{\gamma} \cdot R^2 / D_i$. Equation (13) is valid at steady state, for $t >> \dot{\gamma}^{-1}$. Hence, Equation (13) represents the asymptotic solution. For $t \to 0$, one has $k_L a_{drop} = 4 \cdot R^2 \cdot \sqrt{\pi \cdot D_i / t}$. For $N_{Ca} = 0$, Equation (13) describes mass transfer to or from spherical drops.

The population of droplets was identified using population balance, and it was possible to recalculate the specific interfacial area, *a*, from the surface of deformed droplet a_{drop} and calculate the volumetric mass transfer coefficient $k_L a$ in this manner.

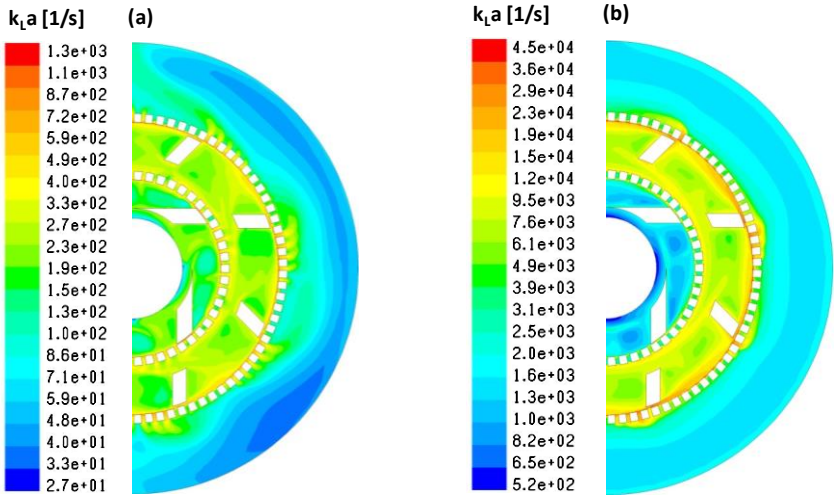

Fig. 9. The volumetric mass transfer coefficient in dense emulsion for $\phi_m = 0.8$, $\phi = 0.75$, $\eta_c = 0.91$ mPas, $\eta_d = 9.4$ mPas, Q = 600 kg/h, for for $N = 1000$ rpm, (b) for $N = 11000$ rpm

Figure 9 shows that there is very large difference in the mass transfer rate between different regions of the rotor-stator mixer. The presented example shows that the new rheological model can be useful for describing interfacial mass transfer as well as the flow of dense emulsion.

4. Possibility of application of rheological model to micelle dispersion

Bouchoux et al. [9] presented measurements of the rheological properties of casein micelle dispersions. They considered three concentration regimes; in the present paper we are interested in the first of these, where the steady shear viscosities were measured with casein micelle dispersions “that flow, i.e., dispersions that do not behave as solids” [9]. For the interpretation of measured viscosity they applied the Krieger and Dougherty model with characteristic stress calculated from

$$\tau_c = \frac{k_B \cdot T}{b \cdot R \cdot T} \tag{14}$$

where k_B is the Boltzmann constant and the average micelle radius R is equal to 100 nm. Parameter b is used for fitting and takes values of between 1 and 3.5. The rate of shear $\dot{\gamma}$ from a range $0.1s^{-1}$ to $1000s^{-1}$ was used in the experiments. The volume fraction of casein micelles was between 0.044 and 0.739. The application of Equation (14) is based on the assumption that the shear is induced by particle thermal fluctuations. Hence, we start by checking if all experiments are in this regime. To this end, we apply the Péclet number defined as follows:

$$Pe = \frac{\dot{\gamma} \cdot R^2}{D_B(\phi)} \tag{15}$$

where $D_B(\phi)$ is the coefficient of Brownian diffusion in suspension of volume fraction ϕ.
If *Pe* exceeds unity, the Brownian motion does not contribute much to viscosity. To calculate *Pe*, the method of Buyevich and Kabpsov [10] is applied.

$$D_B(\phi) = \frac{D_B^{\infty}}{\chi(\phi)} \tag{16}$$

$$\varphi(\phi) = \chi cs(\phi) + 1.08 \cdot \frac{(\phi / \phi_m)}{1 - \phi / \phi_m} \tag{17}$$

$$\chi cs(\phi) = \frac{1 - 0.5 \cdot \phi}{(1 - \phi)^3} \tag{18}$$

Figure 10 shows the effects of the shear rate and micelle volume fraction on *Pe*.

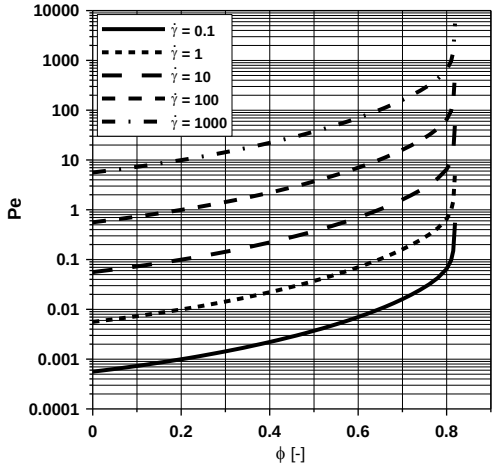

Fig. 10. Effect of micelle volume fraction on *Pe*, $\phi_m = 0.82$

When Equation (4) is presented in the form

$$F(\phi,\dot{\gamma}) = \frac{\eta_r(\phi,\dot{\gamma})}{\left(1-\frac{\phi}{\phi_m}\right)^{-2.5\phi_m}} \tag{19}$$

one can check if there is any non-Brownian regime where the $F(\phi,\dot{\gamma})$ curves collapse. Figure 11 shows that this is the case.

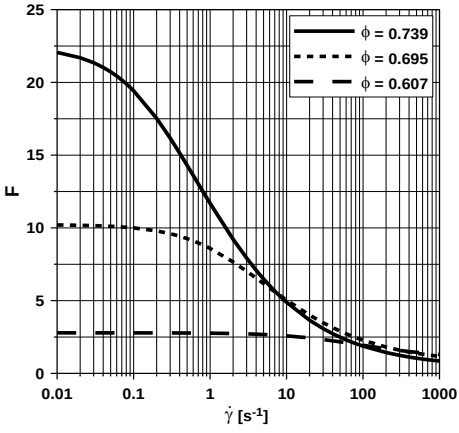

Fig. 11. Effect of shear rate on $F(\phi,\dot{\gamma})$, $\phi_m = 0.82$

Figure 11 shows that both the Brownian and non-Brownian mechanisms should be combined and applied to interpret experimental data properly. This can be done in future by combining the model presented in this work with the model valid for the Brownian regime.

5. Conclusions

In this paper, several new possible applications of the model developed initially to describe rheology of dense emulsions have been presented. These new applications include modelling of the specific interfacial area and the volumetric mass transfer coefficient during the process of emulsion formation and afterwards, during emulsion flow. Another potential application is related to modelling the viscosity of micelle suspensions; the combining of Brownian and non-Brownian mechanisms is proposed for future research.

References

[1] Taylor G. I., *The viscosity of a fluid containing small drops of another liquid*. Proc. R. Soc. London, Ser. A, vol. 138, 1932, 41-48.

[2] Bałdyga, J., Jasińska M., Kowalski A. J., *Effect of rheology of dense emulsions on the flow structure in agitated systems.* Chem. Eng. Res. Des. 2015, http://dx.doi.org/10.1016/j.cherd.2015.11.026

[3] Pal R., *Viscous behavior of concentrated emulsions of two immiscible Newtonian fluids with interfacial tension*, Journal of Colloid and Interface Science, vol. 263, 2003, 296-305.

[4] Bałdyga J. and W. Podgórska, *Drop break-up in intermittent turbulence. Maximum stable and transient sizes of drops*, Can. J. Chem. Eng., vol. 76, 1988, 456-470.

[5] Ovarlez G., Rodts, S., Ragouilliaux A., Coussot P., Goyon J., A. Colin A., *Wide-gap Couette flows of dense emulsions: Local concentration measurements, and comparison between macroscopic and local constitutive law measurements through magnetic resonance imaging*. Physical Review E, vol. 78, 2008, 036307

[6] Jasińska, M., Bałdyga, J., Hall, S., Pacek, A.W., *Dispersion of oil droplets in rotor-stator mixers: Experimental investigations and modeling*, Chemical Engineering and Processing, vol. 84, 2014, 45-53.

[7] Taylor, T. D. and A. Acrivos, *On the deformation and drag of a falling viscous drop at low Reynolds number*, J. Fluid Mech. vol. 18, 1964, 466–476.

[8] Favelukis M. and Lavrenteva O. M., *Mass transfer around prolate spheroidal drops in an extensional flow*. The Canadian Journal of Chemical Engineering, vol. 91, 2013, 1190-1199.

[9] Bouchoux A., Debbou B., Gésan-Guiziou G., Famelart M.-H., Doublier J.-L., Cabane B., *Rheology and phase behavior of dense casein micelle dispersions* The Journal of Chemical Physics, vol. 131, 2009, 65106.

[10] Buyevich Yu.A., Kabpsov S.K., *Segregation of fine suspension in channel flow*, J. Non-Newtonian Fluid Mech., vol. 86, 1999, 157-184.

Acknowledgement

The authors acknowledge financial support from Polish National Science Centre (Grant agreement number: DEC-2013/11/B/ST8/00258).